Fizika Nizkikh Temperatur, 2003, v. 29, Nos. 9/10, p. 1093–1100

Quantum property of solid hydrogen as revealed by high-resolution laser spectroscopy

Hiroyuki Katsuki[1], Mizuho Fushitani[2], and Takamasa Momose

Department of Chemistry, Graduate School of Science, Kyoto University, Kyoto 606-8502, Japan
E-mail: momose@kuchem.kyoto-u.ac.jp

Pure vibrational overtone transitions of solid parahydrogen were studied using high-resolution laser spectroscopy. Extremely narrow spectral linewidth (~20 MHz) allowed us to observe rich spectral structure that originates in subtle intermolecular interactions in the crystal. It was found that anisotropy of the distribution of zero-point lattice vibration of hydrogen molecules perturbs the energy levels of the vibrationally excited states significantly. Large amplitude of the zero-point lattice vibration being an intrinsic nature of quantum solids, was directly observed from the present high-resolution spectroscopy. The first observation of a pure vibrational overtone transition of solid orthodeuterium is also discussed.

PACS: 33.20.Ea, **63.50.+x**, **67.80.–s**

1. Introduction

Optical linewidths of the condensed phase are, in general, two or three orders of magnitude broader than that in the gas phase. The broadness of the linewidths wipes out most spectral information that might give us detailed information on intermolecular interactions and other properties of condensed phases. However, an exception to this generalization was recently found for solid hydrogen crystals [1–3]. Optical transitions of hydrogen crystals in the infrared spectral region are, surprisingly, as narrow as 4 MHz (= 0.00013 cm^{-1}) [4]. The exceptional sharpness of the optical transitions of hydrogen crystals allows us to observe fine spectral structures originating in subtle interactions in the condensed phase, which provides a new methodology to investigate properties of the condensed phase from a microscopic point of view.

Solid hydrogen has been attracting attention not only because it is the simplest and most fundamental molecular crystal [5,6] but also because it is a quantum crystal [7]. Since hydrogen molecules have vibrational and rotational degrees of freedom, studies of solid hydrogen will shed light on different aspects of quantum crystals that can never be obtained from studies of solid He.

One of the important properties of quantum crystals is the large amplitude of zero-point lattice vibration. Due to the small mass of a hydrogen molecule in addition to the weak intermolecular interaction between hydrogen molecules, the mean amplitude of the zero-point lattice vibration of solid hydrogen crystal extends approximately 20 % of the intermolecular distance. The delocalization of the wavefunction of hydrogen molecules in the lattice must affect most properties of the crystal. However, observation of such a quantum effect is difficult and few experimental observations directly related to the quantum effect have been reported so far. High-resolution spectroscopy, then, offers a promising technique to observe the quantum effect directly, because the optical spectra give us greatly detailed microscopic information.

Here, we discuss on the quantum feature of solid hydrogen revealed by high-resolution spectroscopy of pure vibrational overtone transitions. We have observed and analyzed the $Q_2(0)$ ($v = 2 \leftarrow 0$, $J = 0 \leftarrow 0$) and $Q_3(0)$ ($v = 3 \leftarrow 0$, $J = 0 \leftarrow 0$) absorption transitions of solid parahydrogen induced by an impurity orthohydrogen molecule. Since the transitions we have studied are induced by intermolecular interactions, which are a function of the distance between

[1] Present address: Physical Chemistry Institute, University of Zurich, Switzerland

[2] Present address: Institute für Experimentalphysik, Freie Universität Berlin, Germany

molecules, the transition frequencies contain information on the effect of the large amplitude of zero-point lattice vibration. Here, we focus on the quantum property of solid hydrogen obtained form the analysis of the optical spectral structure.

In addition to the $Q_n(0)$ transitions of solid parahydrogen, the first observation of the high-resolution spectrum of the $Q_2(0)$ transition of solid orthodeuterium is also discussed.

2. $Q_n(0)$ transitions of solid hydrogen

The $Q_n(0)$ ($v = n \leftarrow 0, J = 0 \leftarrow 0$) transitions of H_2 and D_2 become optically active when these molecules are placed under an electric field. Due to the polarizability α of hydrogen molecules, an electric field E induces a dipole moment $\mu = \alpha E$ on the hydrogen molecule, which interacts with radiation to cause the $Q_n(0)$ transitions [2,8,9].

The $Q_n(0)$ transitions we have studied here are those induced by the electric field of the averaged quadrupole moment of an impurity $J = 1$ hydrogen molecule in the crystal. Upon the $Q_n(0)$ transitions, the inducer $J = 1$ hydrogen also changes its value of the quantum number M which is the projection of the rotational angular momentum J. Thus, the $Q_n(0)$ transitions we have observed are simultaneous transitions which should be written as $Q_n(0) + Q_0(1)$ [8]. Vibrons produced by the transitions are almost localized near the inducer $J = 1$ hydrogen molecule, contrary to the cases of the Raman [2] and Condon [9] transitions.

The crystal structure of solid parahydrogen and solid orthodeuterium is known to be hexagonal close packed. There are two types of the nearest-neighbor pair between two hydrogen molecules in a crystal of the hexagonal close packed structure. One is the in-plane (IP) pair and the other is the out-of-plane (OP) pair. Figure 1 depicts the 12 nearest neighbor molecules of a $J = 1$ hydrogen molecule in a crystal of the hexagonal close packed structure. Six hydrogen molecules reside on the hexagonal plane, while three hydrogen molecules are above and three molecules are below the plane. The IP pair is a pair between two hydrogen molecules in the same hexagonal plane (Fig. 1(*a*)), and the OP pair is a pair between two hydrogen molecules in a different plane next to each other (Fig. 1 (*b*)). Since the environment around the pair is different between IP and OP pairs, we treat these pairs separately in the following discussion.

The $Q_1(0)$, $Q_2(0)$, and $Q_3(0)$ transitions have been observed at 4,153, 8,070 [10,11], and 11,758 cm^{-1} [12], respectively. We have studied the $Q_2(0)$ and $Q_3(0)$ transitions with higher spectral resolution than previous works to find new, fine splittings of the

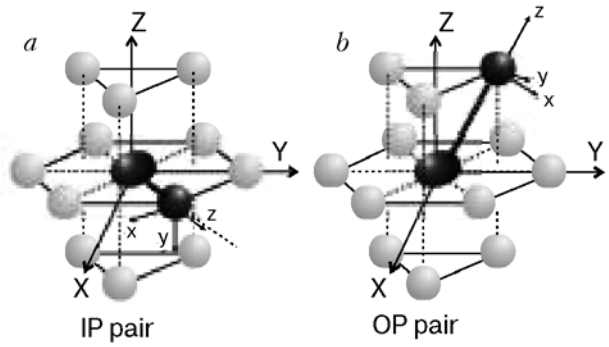

Fig. 1. A $J = 1$ hydrogen molecule (displayed as ellipses) and its twelve nearest neighbor hydrogen molecules in a crystal of the hexagonal close packed structure. (*a*) In-plane (IP) pair configurations. (*b*) Out-of-plane (OP) pair configurations. Molecules in the same basal plane are connected by solid lines. The IP and OP pairs are represented by a bold broken line. The crystal-fixed-axis (XYZ) and the pair-axis (xyz) are also shown. The crystal c axis is the same as the Z axis.

spectra [13,14]. It was concluded that these fine splittings we have observed contain important information on the quantum property of solid hydrogen.

3. Intermolecular interactions in quantum crystals

Before going into details about the experimental results, we will discuss the quantum effect on intermolecular interactions. The effect of the large amplitude of zero-point lattice vibration in solid hydrogen has to be taken into account when interaction between hydrogen molecules is considered. Inclusion of the effect of the zero-point vibration is often referred to as the «renormalization problem», and it has been discussed by Luryi and van Kranendonk in the case of hydrogen crystals [15].

Here we consider intermolecular interaction between $J = 0$ hydrogen and $J = 1$ hydrogen molecules. When the two molecules are fixed at a distance of R_0, the anisotropic interaction between these two molecules is well described as [6,13]

$$V(R_0, \omega_1) = B_0(R_0) C_{2,0}(\omega_1), \qquad (1)$$

where ω_1 is the orientation of the $J = 1$ hydrogen molecule with respect to the axis between two molecules (hereon, the pair-axis). The symbol $C_{l,\mathrm{m}}(\omega)$ expresses the Racah spherical harmonics, which are related to the standard spherical harmonics $Y_{l,m}(\omega)$ as $C_{l,m}(\omega) = \sqrt{4\pi/(2l+1)}\, Y_{l,m}(\omega)$. The coefficient B_0 in Eq. (1) is a function of R_0. The expression in Eq. (1)

is applicable only to the case when two molecules are rigidly fixed at a distance of R_0.

In solid hydrogen, however, zero-point motion of intermolecular vibration is considerably large so that the «instantaneous» position of a molecule displaced from its equilibrium position needs to be explicitly taken into account. According to Luryi and van Kranendonk [15], Eq. (1) should be modified for quantum crystal as

$$\tilde{V}(R_0, \omega_1) = \tilde{B}_0(R_0) C_{2,0}(\omega_1) + \tilde{B}_2(R_0)[C_{2,2}(\omega_1) + C_{2,-2}(\omega_1)], \quad (2)$$

where the intermolecular interaction potential is expanded in terms of the R_0. The coefficients $\tilde{B}_0$ and $\tilde{B}_2$ are the function of the R_0 only. The first term of the right-hand side of Eq. (2) has the same orientational dependence as the right-hand side of Eq. (1). But since the effect of zero-point vibration is renormalized, the tilde is used for the coefficient in Eq. (2) in order to distinguish it from the coefficient in Eq. (1).

The second term of the right-hand side of Eq. (2) originates in the anisotropy of the distribution of the zero-point vibration. More explicitly, when the instantaneous position of the hydrogen molecule relative to the lattice point is described by the **u**, the coefficient $\tilde{B}_2(R_0)$ in Eq. (2) is approximately related to the coefficient $B_0(R_0)$ in Eq. (1) as

$$\tilde{B}_2(R_0) = \frac{\sqrt{6}}{4} \eta B_0(R_0), \quad (3)$$

where η is the nonaxiality parameter defined as

$$\eta = \frac{1}{R_0^2} \left\langle u_x^2 - u_y^2 \right\rangle. \quad (4)$$

The Cartesian components u_x and u_y of the instantaneous vector **u** are those for the pair-axis as shown in Fig. 1.

The physical origin of the second term of the right-hand side of Eq. (2) may become more clear, when we look at the problem from the group theoretical point of view. When the distribution is axially symmetric with respect to the pair-axis, the interaction potential should be described by only the first term of the right-hand side of Eq. (2), because the potential has to be totally symmetric with respect to any symmetry operation along the pair-axis that belongs to the $C_{\infty v}$ point group. However, the distribution may not necessarily be axially symmetric. For example, in the case of the IP pair shown in Fig. 1 (*a*), the distribution of zero-point vibration could be deformed towards the hexagonal plane or elongated toward the *c* axis. Then the potential has to be totally symmetric with respect to any symmetry operation that belongs to the C_{2v} point group. It is also true for the OP pair that the potential has to be totally symmetric in C_{2v}. When we construct symmetry adapted functions of linear combinations of the Racah spherical harmonics up to the second rank, the totally symmetric functions among them (besides $C_{0,0}(\omega)$) in the C_{2v} point group are found to be $C_{2,0}(\omega)$ and $C_{2,2}(\omega) + C_{2,-2}(\omega)$, the latter being the second term of the right-hand side of Eq. (2). Thus, the second term originates in the nonaxiality of the distribution of zero-point vibration relative to the pair-axis. Although both parameters $\tilde{B}_0$ and $\tilde{B}_2$ contain information on the renormalized effect, it should be emphasized that the parameter $\tilde{B}_2$ contains only the pure quantum effect of the solid.

Each hydrogen molecule in solid hydrogen is under the potential which is approximated as a sum of the pair intermolecular interaction from all the surrounding hydrogen molecules. We call this potential the «crystal field potential». For the analysis of the spectra of the $Q_n(0)$ transitions, we only need to consider the interaction potential between an impurity $J = 1$ hydrogen molecule and surrounding parahydrogen molecules [13]. In addition, since the quantum effect shown in Eq. (2) significantly contributes only to the nearest-neighbor pairs but not to distant pairs, Eq. (2) is used for the interaction between nearest neighbor pairs, while Eq. (1) is used for further distant pairs in the present analysis.

Because of the difference of the polarizability of hydrogen molecules in different vibrational states, the crystal field potential has to be considered separately between the ground state and the vibrationally excited states. When all the $J = 0$ hydrogen molecules are in the ground state, the crystal field potential is found to be

$$V^{\mathrm{gr}}(\Omega, R_0) = \varepsilon_{2c} C_{2,0}(\Omega). \quad (5)$$

The coefficient ε_{2c} is called the crystal field parameter. In order to derive Eq. (5), we used the relation of $C_{2,m}(\omega_1) = \sum_n D^2_{n,m}(\mathcal{R}) C_{2,n}(\Omega)$ to change the axis system from the pair-axis to the crystal-fixed axis (see Fig. 1), where Ω is the orientation of the $J = 1$ molecule relative to the crystal-fixed axis and $\mathcal{R}$ is the orientation of the pair-axis with respect to the crystal-fixed axis. The function $D^2_{n,m}(\mathcal{R})$ is the Wigner rotation matrix [16]. In Eq. (5), only the term proportional to $C_{2,0}(\Omega)$ remains although we used Eq. (2) for the nearest neighboring pairs. Terms other than $C_{2,0}(\Omega)$ vanish because of the symmetry of the crystal (D_{3h}) around the central hydrogen molecule.

When one of the parahydrogen molecules is in the vibrationally excited state, the crystal field potential becomes more complex than Eq. (5). We express the

crystal field potential of the vibrationally excited states as a sum of the crystal field potential of the ground state (Eq. (5)) and the correction terms due to the excitation. When the jth hydrogen molecule is excited to its vibrationally excited state, the crystal field potential of such expression becomes,

$$V^{\mathrm{ex}}(\Omega, R_0) = \varepsilon_{2c} C_{2,0}(\Omega) +$$

$$+ \Delta\tilde{B}_0 \sum_{m'=-2}^{2} D^2_{m',0}(\mathcal{R}_j) D^{2*}_{m',0}(\Omega) +$$

$$+ \Delta\tilde{B}_2 \sum_{m'=-2}^{2} [D^2_{m',2}(\mathcal{R}_j) + D^2_{m',-2}(\mathcal{R}_j)] D^{2*}_{m',0}(\Omega), \quad (6)$$

where the first term of the right-hand side is the ground state crystal field potential, and the second and third terms express the correction due to the vibrational excitation. The symbol $\mathcal{R}_j$ is the Euler angle of the pair-axis between the jth hydrogen molecule and the central $J = 1$ hydrogen molecule relative to the crystal-fixed axis. The symbol $\Delta\tilde{B}_n$ ($n = 0$ or 2) represents $\tilde{B}_n^{\mathrm{ex}} - \tilde{B}_n$, where $\tilde{B}_n^{\mathrm{ex}}$ is the coefficient of the pair interaction potential in Eq. (2) between the vibrationally excited $J = 0$ hydrogen molecule and the ground $J = 1$ hydrogen molecule. It should be noted that the parameter $\Delta\tilde{B}_2$ related to the pure quantum effect appears explicitly in Eq. (6). In other words, the determination of the parameter $\Delta\tilde{B}_2$ corresponds to the direct observation of the quantum effect of solid hydrogen.

4. Experiments

Parahydrogen crystals were grown by the same method as described previously [13,17]. Briefly, pure parahydrogen gas prepared using a ferric oxide catalyst [17] was continuously introduced in an optical cell kept at about 8 K to grow transparent crystals. The cell was made of copper with both ends sealed with BaF_2 windows with indium gaskets. The size of the cell was 5 cm long and 2 cm in diameter. The concentration of orthohydrogen in the crystal was estimated to be less than 0.01 %. In order to observe the $Q_3(0)$ transition, which is about two orders of magnitude weaker than the $Q_2(0)$ transition, the concentration of orthohydrogen was increased up to 0.1 %.

Orthodeuterium crystals were prepared using a method similar to the one described above [18]. The conversion of paradeuterium to orthodeuterium was carried out with the ferric oxide catalyst kept at 18 K. The crystals were grown at 10.5 K as well. The concentration of paradeuterium was estimated to be around 0.25 %.

The high-resolution spectra of the $Q_2(0)$ transitions of both parahydrogen and orthodeuterium crystals were observed using a difference frequency laser system developed in our laboratory [19]. The $Q_3(0)$ transition was observed using a ring type Ti:sapphire laser. The spectral purity of both laser systems was better than a few MHz (= 10^{-4} cm^{-1}). The tone burst modulation technique was used for sensitive detection [20,21]. All the measurements were done at 4.8 K.

5. $Q_2(0)$ and $Q_3(0)$ transitions of solid parahydrogen

5.1. Observed spectra

Figure 2 shows the observed spectra of the $Q_2(0)$ and the $Q_3(0)$ transitions of solid parahydrogen. Panels (*a*) and (*b*) show the absorption spectra with the polarization of light parallel to the *c* axis and with the polarization perpendicular, respectively. Panels (*c*) and (*d*) show the $Q_3(0)$ spectra with the polarization parallel and perpendicular, respectively. In both transitions, the spectral shapes appear as a second derivative type because of the tone-burst modulation technique. The differences in the intensities of each transition between panels (*a*) and (*b*) and between panels (*c*) and (*d*) in Fig. 2 clearly show that each transition has definite polarization dependence relative to the crystal-fixed axis.

The $Q_2(0)$ spectrum is roughly split into a doublet with a spacing of 0.30 cm^{-1}. Each component exhibits further fine splittings; the lower frequency component shows eight lines, while the higher displays ten. On the other hand, the $Q_3(0)$ spectrum is roughly split into a doublet with a spacing of 0.45 cm^{-1}. Similar spectral structure was also observed in the $Q_3(0)$ transition, but the number of fine splittings in each component is smaller in the $Q_3(0)$ transitions than in $Q_2(0)$; the lower frequency component shows four lines, while the higher component exhibits six.

Previously, Dickson et al. [12] observed roughly the same spectral structure in the $Q_3(0)$ transition as shown in panels (*c*) and (*d*) of Fig. 2. Their spectrum, however, showed a much broader linewidth than ours. The linewidth (FWHM) of each transition shown in Fig. 2 (*c*) and (*d*) is about 30 MHz, which is less than one third of the width observed previously. The narrower spectral linewidth is due to the lower orthohydrogen concentration in our sample. The sharp linewidth allowed us to resolve all the fine splittings in the $Q_3(0)$ transition clearly.

5.2. Analysis

The theoretical framework for the analysis of the $Q_n(0)$ transition was discussed in a previous paper

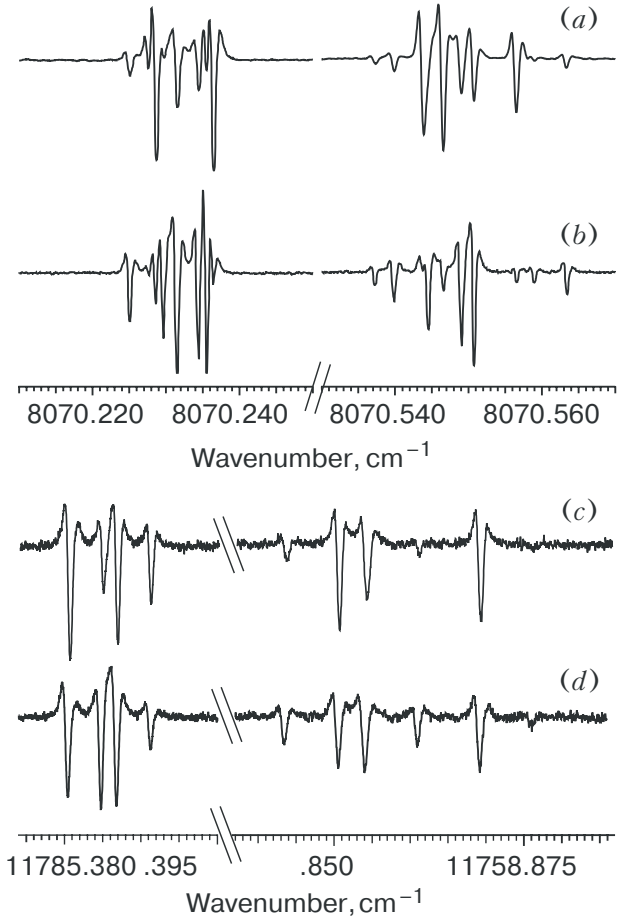

Fig. 2. (*a*) and (*b*): The $Q_2(0)$ transition of solid parahydrogen. The polarization of light is parallel (*a*) and perpendicular (*b*), respectively. (*c*) and (*d*): The $Q_3(0)$ transition of solid parahydrogen. The polarization of light is parallel (*c*) and perpendicular (*d*), respectively. The spectral shapes appear as a second derivative type because of the tone-burst modulation technique.

[13]. Briefly, the Hamiltonian H for the analysis consists of four terms; $H = H_{rv} + V_{\text{crystal}} + H_{\text{hop}} + V_{\text{Stark}}$. The first term is the standard rotation-vibration Hamiltonian of hydrogen molecules, the second terms is the crystal field potential, the third term is the vibron hopping Hamiltonian, and the last term is the Stark potential of the quadrupolar field of the central $J = 1$ hydrogen.

As for the crystal field potential, Eqs. (5) and (6) were used to describe the ground and vibrationally excited state, respectively. In addition, since there are two different pairs in the crystal, different parameters of both $\Delta\tilde{B}_0$ and $\Delta\tilde{B}_2$ were employed for IP and OP pairs. These are designated as $\Delta\tilde{B}_0$ (IP) and $\Delta\tilde{B}_2$ (IP) for the IP pair, and $\Delta\tilde{B}_0$ (OP) and $\Delta\tilde{B}_2$ (OP) for the OP pair.

The vibron hopping Hamiltonian H_{hop} is responsible for the delocalization of the vibrational excited states in the crystal. In the previous paper [13] we found that the $Q_2(0)$ spectrum could not be properly interpreted without the vibron hopping effect. The hopping frequency is designated as σ. On the other hand, the hopping in the $v = 3$ vibrationally excited state is estimated to be negligibly small.

The Stark field potential V_{Stark} arises from the electric field of the $J = 1$ hydrogen molecule. A quantitative discussion of the Stark energy is given in Ref. 13.

The observed transition frequencies were fitted employing the standard least-squares fitting method with the use of a total of six parameters, ε_{2c}, $\Delta\tilde{B}_0$ (IP), $\Delta\tilde{B}_0$ (OP), $\Delta\tilde{B}_2$ (IP), $\Delta\tilde{B}_2$ (OP), and σ. The fitting calculation was performed separately for the $Q_2(0)$ and $Q_3(0)$ transitions. The best fitted parameters are listed in Table.

Table

Crystal field parameters and vibron hopping frequency of the $Q_2(0)$ and $Q_3(0)$ transitions (in cm^{-1})

Parameter	$Q_2(0)$	$Q_3(0)$
ε_{2c}	−0.0116(2)	−0.0112(2)
$\Delta\tilde{B}_0$ (IP)	−0.5278(5)	−0.7879(4)
$\Delta\tilde{B}_0$ (OP)	−0.5287(5)	−0.7880(3)
$\Delta\tilde{B}_2$ (IP)	−0.0045(2)	−0.0069(3)
$\Delta\tilde{B}_2$ (OP)	0.0149(3)	0.0236(2)
σ	−0.0038(1)	0.0

5.3. Crystal field potential

Although the parameters for the $Q_2(0)$ and $Q_3(0)$ transitions were calculated separately, the agreement of the crystal field parameter ε_{2c} between these two transitions is noteworthy. The parameter gives the crystal field splitting of

$$\delta_1 = E(M = \pm 1) - E(M = 0) = -0.6\varepsilon_{2c} \qquad (7)$$

for an orthohydrogen molecule in pure parahydrogen crystal.

Determination of the value and sign of δ_1 has been attracting much attention because it may explain the anomalous behavior of the specific heat of solid parahydrogen [6,22]. The most accurate value of δ_1 so far reported is 0.0071 cm^{-1} by Dickson et al. [12]. Our experimental results support their value. Since our spectral resolution was much better than the previous experiment [12], our parameter must be more

accurate than theirs. From our observations we conclude that the $M = \pm 1$ level is above the $M = 0$ level and the separation is (0.00696 ± 0.00012) cm^{-1} = = (10.01 ± 0.17) mK.

5.4. Quantum effect

As discussed above, the parameter $\Delta\tilde{B}_2$ originates in the pure quantum effect. Although the absolute values of the $\Delta\tilde{B}_2$ determined are small, they play a significant contribution to the energy levels of the vibrationally excited states. In order to observe the effect of the parameter $\Delta\tilde{B}_2$ in detail, we also performed the fitting calculation without the parameter $\Delta\tilde{B}_2$. Figure 3 compares the calculated results with the observed spectrum. Panel (*a*) shows the calculated frequencies of the $Q_3(0)$ transition using only three parameters ε_{2c}, $\Delta\tilde{B}_0$ (IP), and $\Delta\tilde{B}_0$ (OP) for the fitting, while panel (*b*) shows the frequencies calculated using all of the five parameters ε_{2c}, $\Delta\tilde{B}_0$ (IP), $\Delta\tilde{B}_0$ (OP), $\Delta\tilde{B}_2$ (IP), and $\Delta\tilde{B}_2$ (OP). (The vibron hopping frequency σ was fixed at zero.) Panel (*c*) shows the observed spectrum. It is clear from panels (*a*) and (*b*) compared to panel (*c*) that the inclusion of the parameter $\Delta\tilde{B}_2$ is essential for the quantitative analysis of the observed spectrum. In other words, the quantum effect is directly observed in the $Q_n(0)$ spectrum.

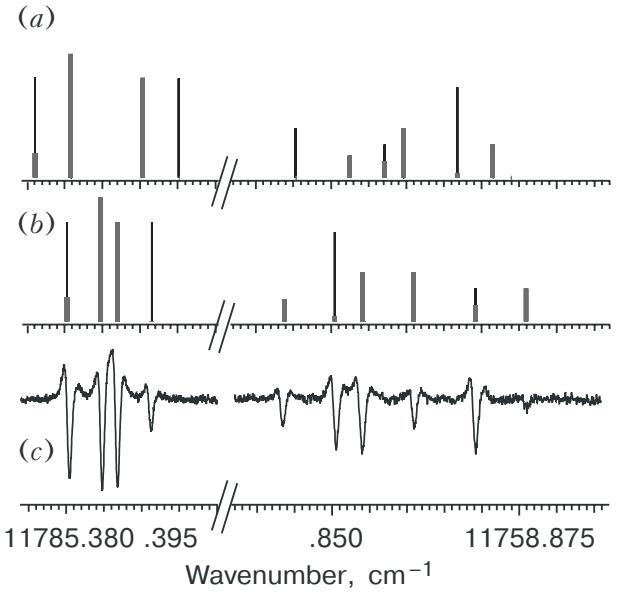

Fig. 3. (*a*) Calculated $Q_3(0)$ transition frequencies without using the quantum parameter ΔB_2 for the fitting. The best fitted parameters are $\varepsilon_{2c} = -0.0238$ cm^{-1}, $\Delta\tilde{B}_0$ (IP) = = -0.7980 cm^{-1}, and $\Delta\tilde{B}_0$ (OP) = -0.7858 cm^{-1}. The bold lines show the perpendicular transitions, while the thin lines show parallel transitions. (*b*) Calculated frequencies with the use of all of the five parameters. The parameters are give in Table. (*c*) Observed $Q_3(0)$ spectrum (same as Fig. 2 (*d*)).

From Table, we see significant difference of the parameter $\Delta\tilde{B}_2$ between the IP and OP pairs. This difference must be related to the difference of nonaxiality parameter η in Eq. (4). It has been discussed by Luryi and van Kranendonk [15] that the nonaxiality parameters for the IP pair (η (IP)) and the OP pair (η (OP)) are related and expressed as $\eta(\mathrm{IP})/\eta(\mathrm{OP}) = -1/3$. From the analysis of our spectrum, we obtained the ratio of $|\Delta\tilde{B}_2(\mathrm{IP})/\Delta\tilde{B}_2(\mathrm{OP})| = 0.30$. Since our ratio is not the ratio $\tilde{B}_2(\mathrm{IP})/\tilde{B}_2(\mathrm{OP})$ of the ground state, but the ratio of the difference of the parameter $\tilde{B}_2$ between the vibrationally excited state and the ground state, our ratio of $|\Delta\tilde{B}_2(\mathrm{IP})/\Delta\tilde{B}_2(\mathrm{OP})| = 0.30$ can not be compared directly with the ratio of $\eta(\mathrm{IP})/\eta(\mathrm{OP}) = -1/3$. But the similarity is worth noting.

The parameter $\Delta\tilde{B}_0$ contains more complicated quantum effect than the parameter $\Delta\tilde{B}_2$ [13], and we do not discuss this here. We just mention that the parameter $\Delta\tilde{B}_0$ is found to be very close between the IP pairs and OP pairs. More detailed discussion on the parameters shown in Table is given in a separate paper [14].

6. $Q_2(0)$ transition of solid orthodeuterium

It has been shown that there are remarkable differences in the behaviors of solid H_2 and solid D_2 [5]. Some of the differences have come to be well understood — such as slower ortho-para conversion in solid D_2 than in solid H_2, and slower quantum diffusion in solid D_2. But there are still some puzzling differences between them. For example, the fact that impurity $J = 1$ pairs show sharp NMR lines in solid H_2, but not in solid D_2 is yet to be understood [23,24].

Since the high-resolution spectroscopic technique is a powerful method for investigating properties of solid hydrogen from a macroscopic point of view, application of the technique to solid orthodeuterium is worth trying. As a first step of such research, we observed the high-resolution spectrum of the $Q_2(0)$ transition of solid orthodeuterium for the first time.

Figure 4 shows the observed $Q_2(0)$ transition of solid orthodeuterium. Tone-burst modulation technique was employed herein. A doublet with a spacing of 0.27 cm^{-1} was observed. The doublet corresponds to the doublet with a spacing of 0.30 cm^{-1} of the $Q_2(0)$ transition of solid parahydrogen shown in Fig. 2 (*a*) and (*b*). The linewidth of the doublet in Fig. 4 is about 300 MHz (= 0.01 cm^{-1}). We could not resolve any further splitting in each component as is seen in Fig. 2, contrary to the case of the $Q_2(0)$ transition of solid parahydrogen. The broad linewidth is mostly due to a higher $J = 1$ concentration in solid orthodeuterium (0.25 %) than in solid parahydrogen (0.01 %).

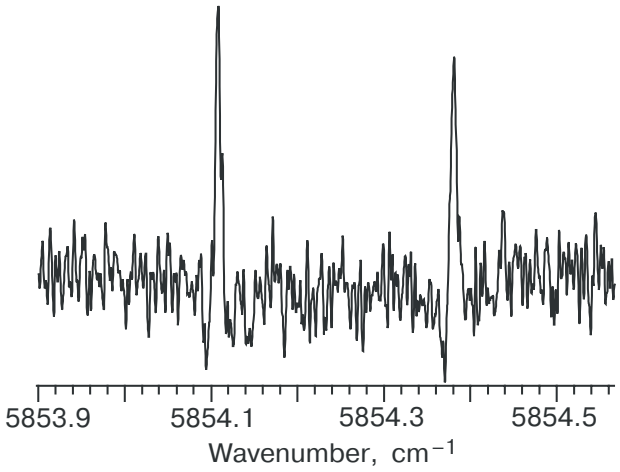

Fig. 4. The $Q_2(0)$ transition of solid orthodeuterium. The concentration of paradeuterium is estimated to be 0.25 %.

The doublet originates in the splitting between $M = 0$ and $M = \pm 1$ in the $v = 2$ excited state. From the spacing of 0.27 cm^{-1}, we estimate the crystal field parameter ΔB_0 to be 0.45 cm^{-1} for solid orthodeuterium [4]. The ratio of ΔB_0 between solid D_2 and solid H_2 for the $Q_2(0)$ transition $\Delta B_0^{D_2} / \Delta B_0^{H_2}$ is roughly 0.85.

Since the intermolecular interaction between hydrogen molecules originates in the dispersion interaction, the coefficient B_0 in Eq. (2) is, as a first order approximation, roughly proportional to $\gamma_{J=1}\alpha_{J=0,v} / R^6$ where $\gamma_{J=1}$ is the anisotropic polarizability of the $J = 1$ hydrogen molecule, $\alpha_{J=0,n}$ is the isotropic polarizability of $J = 0$ hydrogen molecule in the $v = n$ vibrational state, and R is the distance between two molecules. By referring to the theoretically calculated polarizabilities [25], the ratio $\Delta B_0^{D_2} / \Delta B_0^{H_2}$ is calculated to be around 0.9, which is in good agreement with the observed value of 0.85.

Since no further splitting is observed in each component of the doublet, we conclude that the ground state crystal field splitting δ_1 of solid orthodeuterium is less than the width; that is, 0.01 cm^{-1}. In order to determine the crystal field parameter accurately as in the case of solid parahydrogen, we need to reduce the concentration of paradeuterium in our crystal. Such work is now underway.

7. Conclusion

In this paper, we discussed the quantum property of solid hydrogen which is obtainable from high-resolution spectroscopy of the rotation-vibration transitions of hydrogen molecules. It was demonstrated that the large amplitude of zero-point lattice vibration modifies the energy levels of the vibrational excited states significantly, which were clearly observed using high-resolution spectroscopy. Further studies with this high-resolution technique will give us more information on the nature of quantum solids, which are otherwise difficult to obtain.

Acknowledgments

The work described herein was supported in part by the Grant-in Aid for Scientific Research of the Ministry of Education, Science, Culture, and Sports of Japan. The authors would like to thank Prof. H. Meyer who drew our attention to the problems of solid deuterium. Further, H. Katsuki would also like to acknowledge the support from JSPS Research Fellowships for Young Scientists.

1. M. Okumura, M.C. Chan, and T. Oka, *Phys. Rev. Lett*. **62**, 32 (1989).
2. T. Momose, D.P. Weliky, and T. Oka, *J. Mol. Spectrosc*. **153**, 760 (1992).
3. T. Oka, *Annu. Rev. Phys. Chem*. **44**, 299 (1993).
4. D.P. Weliky, K.E. Kerr, T.J. Byers, Y. Zhang, T. Momose, and T. Oka, *J. Chem. Phys*. **105**, 4461 (1996).
5. F. Silvera, *Rev. Mod. Phys*. **52**, 393 (1980).
6. J. van Kranendonk, *Solid Hydrogen, Theory of the Properties of Solid* H_2, HD, *and* D_2, Plenum, New York (1983).
7. L.H. Nosanow, *Phys. Rev*. **146**, 120 (1966).
8. V.F. Sears and J. van Kranendonk, *Can. J. Phys*. **42**, 980 (1964).
9. K.E. Kerr, T. Momose, D.P. Weliky, C.M. Gabrys, and T. Oka, *Phys. Rev. Lett*. **72**, 3957 (1994).
10. D.P. Weliky, T.J. Byers, K.E. Kerr, T. Momose, R.M. Dickson, and T. Oka, *Appl. Phys. B: Lasers Opt*. **59**, 265 (1994).
11. M. Mengel, B.P. Winnewisser, and M. Winnewisser, *Phys. Rev*. **B55**, 10420 (1997).
12. R.M. Dickson, T. Momose, T.J. Byers, and T. Oka, *Phys. Rev*. **B57**, 941 (1998).
13. H. Katsuki and T. Momose, *J. Chem. Phys*. **116**, 8881 (2002).
14. H. Katsuki and T. Momose, to be submitted.
15. S. Luryi and J. van Kranendonk, *Can. J. Phys*. **57**, 136 (1979); *ibid*. 307 (1979); *ibid*. 933 (1979).
16. M.E. Rose, *Elementary Theory of Angular Momentum*, John Wiley & Sons, Inc., New York (1957).
17. T. Momose and T. Shida, *Bull. Chem. Soc. Jpn*. **71**, 1 (1998).
18. H. Hoshina, M. Fushitani, and T. Momose, *J. Chem. Phys*., to be submitted.
19. T. Momose, T. Wakabayashi, and T. Shida, *J. Opt. Soc. Am*. **B13**, 1706 (1996).
20. H.M. Pickett, *Appl. Opt*. **19**, 2745 (1980).
21. C.S. Gudeman, M.H. Begemann, J. Pfaff, and R.J. Saykally, *Opt. Lett*. **8**, 310 (1983).

22. T. Nakamura, *Prog. Theor. Phys*. (Kyoto) **14**, 135 (1955).
23. M. Calkins, R. Banke, X. Li, and H. Meyer, *J. Low Temp. Phys*. **65**, 47 (1986).
24. A.B. Harris, H. Meyer, and X. Quin, *Phys, Rev*. **B49**, 3844 (1994).
25. W. Kolos and L. Wolniewicz, *J. Chem. Phys*. **46**, 1426 (1967).